

illuminated at normal incidence with outer-space sunlight. This thrust level can be increased by electrical heating, by increasing the exposed area, or by causing the material to sublime through a nozzle. There is considerable merit in the use of a low-thrust, long time source of impulse for station-keeping of a comparatively fragile satellite, such as a gravity-gradient stabilized satellite in a synchronous orbit. Another possible use would be in the control of spin rate by mounting one of these devices so that its direction of thrust would have a long moment arm with respect to the center of mass of the satellite.

Conclusions

Subliming materials can be utilized for performing a large variety of functions to increase the effectiveness of a spacecraft mission. These mechanisms can be made extremely light, simple, and highly reliable. Several subliming materials investigated for this purpose provide a wide variance in actuation times. Mixtures of these materials can be used to

obtain virtually any sublimation rate that might be desired. A record of 100% reliability has been established in using these devices on many different earth satellites.

References

- ¹ Perry, J. H., *Chemical Engineer's Handbook* (McGraw Hill Book Co., Inc., New York, 1941), 2nd ed.
- ² Hertz, H., "Ueber die Verdunstung der Flüssigkeiten Insbesondere des Quecksilbers, im Luftleeren Raume," *Ann. Physik* 17, 177 (1882).
- ³ Glasstone, S. and Taylor, H., *Treatise on Physical Chemistry: Atomistics and Thermodynamics* (D. Van Nostrand Co., Inc., Princeton, N. J., 1942), Vol. I.
- ⁴ *Handbook of Chemistry and Physics* (Chemical Rubber Publishing Co., Cleveland, Ohio, 1940-1941), 24th ed., pp. 1794-1799.
- ⁵ Paul, B., "Compilation of evaporation coefficients," *ARS J.* 32, 1321-1328 (1962).
- ⁶ Fischell, R. E. and Mobley, F. F., "A system for passive gravity-gradient stabilization of earth satellites," Johns Hopkins Univ., Applied Physics Lab. Rept. TG-514 (August 1963).

MAY-JUNE 1965

J. SPACECRAFT

VOL. 2, NO. 3

Space Engine Performance Prediction

F. X. McKEVITT* AND T. J. WALSH†
Aerojet-General Corporation, Sacramento, Calif.

In-space engines, typified by low chamber pressures and high expansion ratios, undergo the major part of their development at sea level. Correct inference of combustion efficiency from sea-level test data and accurate prediction of vacuum thrust coefficients are therefore essential to satisfactory system development. An experimental technique was developed for determining nozzle stagnation pressure and hence combustion efficiency from measured thrust rather than from injector face pressure. This method requires the use of a low area-ratio nozzle of known thrust coefficient. Nozzle divergence losses are based on the ratio of thrust coefficients found by using the axisymmetric method of characteristics to those given by ideal one-dimensional flows; frictional losses are found by integration of wall shear drag for this family of nozzles; and nonequilibrium efficiencies are derived by using the sudden-freezing analysis of K. N. C. Bray. A method of combining these factors to establish over-all performance is presented. Experimental data for both sea-level and simulated altitude-firing tests of liquid rocket engines agree well with the predicted values.

Nomenclature

a = constant in reaction rate constant equation
 A = area, in.²
 b = constant in reaction rate constant equation
 B = $|R_f/X_f|$
 c = constant in reaction rate constant equation
 c^* = characteristic velocity, fps
 C_D = discharge coefficient
 C_f = skin-friction coefficient
 C_F = thrust coefficient
 C_{eD} = drag loss
 C_{eG} = geometry loss
 C_{eK} = chemical dissociation loss
 F = thrust, lbf
 F_w = shear drag, lbf

g = 32.174 ft/sec²
 I_{sp} = specific impulse, lbf-sec/lbm
 k_f = forward reaction rate constant of the freezing reaction, ft⁶/lb-mole²-sec
 M = Mach number
 P = pressure, psia
 R = gas constant, 1545 ft-lbf/lb-mole-°R
 Re = Reynolds number
 R_f = forward reaction rate of the freezing reaction, lb-mole/ft³-sec
 R_t = throat radius, in.
 s = distance along nozzle contour, ft
 T = temperature, °R
 v_{ir}' = stoichiometric coefficient, i th reactant in the r th chemical reaction
 v_{ir}'' = stoichiometric coefficient, i th product in the r th chemical reaction
 V = velocity, fps
 w = viscosity exponent
 \dot{w} = mass flow rate, lb/sec
 W_T = total molecular weight
 x = distance along nozzle axis, ft
 X = difference between forward and backward reaction rates, lb-mole/ft³-sec

Presented as Preprint 64-267 at the 1st AIAA Annual Meeting, Washington, D. C., June 29-July 2, 1964; revision received October 15, 1964. The material reported herein is based on a portion of a study sponsored by NASA under Contract No. NAS 7-136.

* Manager, Space Systems Integration Department.

† Design Engineer, Space Systems Integration Department.

- γ = ratio of specific heats
 γ_i = mole fraction of i th species
 ϵ = nozzle area ratio
 η_c = combustion efficiency
 η_N = nozzle efficiency
 μ = dynamic viscosity, lbm/fps
 ρ = density, lbm/ft³
 τ_w = shearing stress, psi

Subscripts

- a = ambient conditions
 c = chamber or total condition
 e = nozzle exit
 I = ideal value
 inj = injector face
 t = nozzle throat
 eff = effective

Engine Performance Analysis

It is common practice in the rocket industry to define over-all engine efficiency in terms of a combustion efficiency and a nozzle efficiency, which are referred to assumed ideal processes. However, the definitions of the efficiencies and parameters, such as thrust coefficient and characteristic velocity, vary somewhat, although most of them degenerate to a common definition as the ideal state is approached. The primary purpose of the following discussion is to clarify the definitions when deviations from ideal occur.

The ideal values (denoted by subscript I) of specific impulse, thrust coefficient, etc., are derived from computations for the operating parameters (chamber pressure, mixture ratio, and propellant combination) based on the following assumptions: 1) chemical equilibrium is maintained among the combustion products throughout the rocket nozzle; 2) the ideal gas law holds for all gases; 3) the flow of gases throughout the nozzle expansion is isentropic; 4) the incoming propellants burn to completion in an infinite-area chamber at one pressure; 5) the mixture of combustion products is homogeneous, and the flow is uniform and parallel in the chamber and at any cross section in the nozzle; and 6) for any given propellant combination, the possible combustion products can be assumed beforehand from the atomic species present.

Ideal specific impulse is given in Fig. 1 as a function of expansion area ratio, chamber pressure, and propellant mixture ratio for a typical storable propellant $N_2O_4/[0.5 N_2H_4 + 0.5 \text{ unsymmetrical dimethyl hydrazine (UDMH)}]$. The ideal values of characteristic velocity and the effect of sudden freezing of the chemical composition of the nozzle flow at arbitrary values of area ratio are also given in this figure.

The following definitions for engine performance parameters are used throughout:

$$I_{sp} = F/\dot{w} \quad (1)$$

$$C_D = \dot{w}/\dot{w}_I = A_{t, eff}/A_t \quad (2)$$

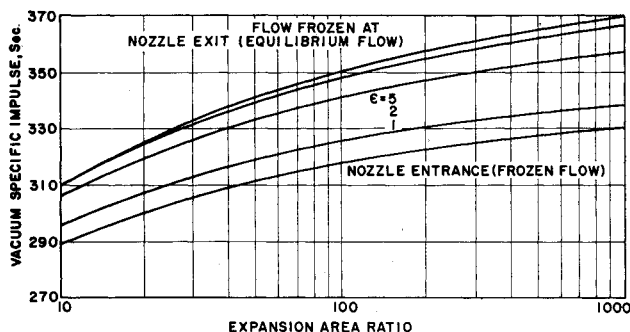


Fig. 1 Specific impulse of $N_2O_4/0.5 N_2H_4 + 0.5$ UDMH for equilibrium and sudden frozen flows, $MR = 2.0$, $P_c = 100$.

$$C_F = F/P_c A_{t, eff} \quad (3)$$

$$c^* = g P_c A_{t, eff}/\dot{w} \quad (4)$$

$$\eta_N = C_F/C_{F, I} \quad (5)$$

$$\eta_c = c^*/c_I^* \quad (6)$$

Choice of the preceding definitions results in several desirable characteristics. The nozzle and combustion efficiencies η_N and η_c are never greater than unity, and the actual specific impulse is related to the ideal specific impulse by the product of the efficiencies

$$I_{sp} = \eta_N \eta_c I_{sp, I} \quad \eta_N \leq 1 \quad \eta_c \leq 1 \quad (7)$$

Also, the familiar relation $I_{sp} = C_F c^*/g$ is preserved.

Normally, actual data and ideal calculations are compared at the same chamber pressure, propellant mixture ratio, and area ratio. However, two interesting conclusions result from manipulation of the previous definitions and relationships. The ideal characteristic velocity is defined from the thermochemical calculation as

$$c_I^* = g P_{c, I}/(\rho V)_I^* \quad (8)$$

where $P_{c, I}$ is the infinite-area chamber pressure, and $(\rho V)_I^*$ is the mass flux at the throat for the ideal case. Then

$$\eta_c = c^*/c_I^* = P_c/P_{c, I} \quad (\rho V)_I^* A_{t, eff}/\dot{w} = P_c/P_{c, I} \quad (9)$$

Thus the combustion efficiency is the ratio of actual nozzle stagnation pressure to the infinite-area equilibrium value of the chamber pressure.

As can be seen, selection of equal chamber pressure between actual and ideal is not strictly a correct reference and, in general, the reference or ideal should be chosen such that the following is satisfied:

$$\dot{w} = (\rho V)_I^* A_{t, eff} = (\rho V)_I^* C_{D, I} A_t \quad (10)$$

or

$$(\rho V)_I^* = \dot{w}/C_{D, I} A_t \quad (11)$$

With this reference, $P_{c, I}$ is always greater than P_c , and the ratio is equal to the combustion efficiency. In practice, such a reference would be difficult to apply, because η_c must be known before the reference calculations can be made, and a trial and error process must be used to find the reference conditions.

Thrust can be expressed by

$$F = \dot{w} V_e/g + P_e A_e = C_F P_c A_t C_D \quad (12)$$

so that

$$C_F = (\dot{w} V_e/g P_c A_t C_D) + (P_e A_e/P_c A_t C_D) \quad (13)$$

It follows that a reference ideal thrust coefficient, which is more suitable than one corresponding to the geometric area ratio is one corresponding to the effective area ratio, which is

$$\epsilon_{eff} = A_e/A_t C_D = \epsilon/C_D \quad (14)$$

Estimation of Nozzle Efficiency

In order to estimate over-all nozzle efficiency, several types of losses are assumed to occur in the nozzle. These losses are assumed to occur independently of each other and hence are referred to the ideal thrust coefficient of the nozzle. The sum of these losses is then the total nozzle inefficiency. Losses considered are those caused by the geometrical shape of the nozzle C_{eG} , viscous friction on the nozzle walls C_{eD} , and failure of all of the dissociated chemical species to recombine in the nozzle C_{eK} . Over-all nozzle efficiency is then given by the following relation:

$$\eta_N = 1 - (C_{eG} + C_{eD} + C_{eK}) \quad (15)$$

and actual thrust coefficient by:

$$C_F = \eta_N C_{F, I} \quad (16)$$

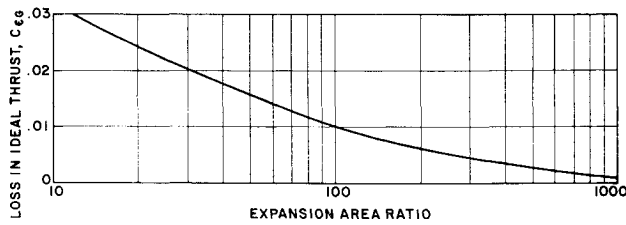


Fig. 2 Effect of geometry on ideal performance of a bell nozzle, $\gamma = 1.2$.

Curves of these loss coefficients are presented in Figs. 2-4. Detailed discussion of the techniques used in obtaining these data are given in the sections that follow. A complete curve showing total losses and distribution is given in Fig. 5. Note that nozzle efficiency is limited to about 94%.

Geometry Loss Factor

A loss results because a practical rocket nozzle contour does not produce uniform parallel exit flow, even with the assumption of an ideal inviscid fluid. Care has been taken to separate out the thrust loss caused by flow restriction at the throat (discharge coefficient), and to charge as a loss only the effect of flow divergence, which would result in an actual reduction in specific impulse.

The nozzle contour optimization that was used for the data presented is that of Rao,¹ in which the maximum thrust contour for a specified nozzle length and ambient pressure is selected. Ambient pressure was assumed to be zero. The solution of the variational problem yields the flow properties on the control surface, and the nozzle contour is constructed by the method of characteristics to give this flow. The flow in the region of the throat is treated using Sauer's method.² Thrust is computed by summing the axial components of the pressure and momentum forces. The geometry loss factor is then obtained as

$$C_{eG} = 1 - F/(C_D F_I) = 1 - I_{sp}/I_{sp,i} \quad (17)$$

A plot of C_{eG} vs area ratio is given in Fig. 2.

Frictional Drag

Losses in thrust incurred by the action of viscous forces at the nozzle wall were evaluated by summing the axial components of the shear drag along the nozzle contour. These losses are expressed as a percent of the ideal, inviscid fluid thrust.

The extended Frankl-Voishel expression for average skin-friction coefficient³ was used

$$C_f = 0.472(\log_{10} Re)^{-2.58} \{1 + [(\gamma - 1)/2]M^2\}^{-0.467} \quad (18)$$

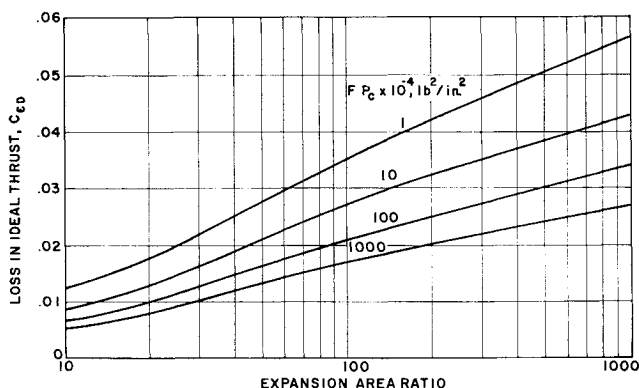


Fig. 3 Effect of shear drag on the ideal performance of a bell nozzle, propellant: $N_2O_4/A-50$, $MR = 2.0$, $\gamma = 1.225$.

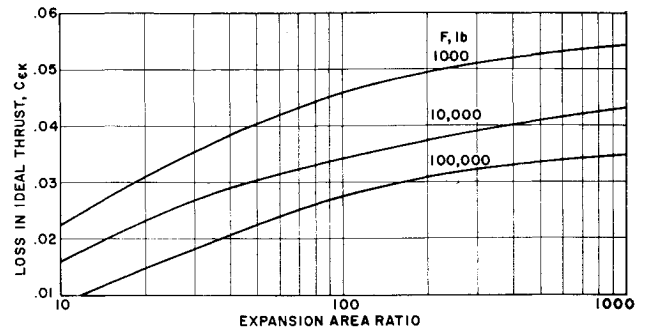


Fig. 4 Effect of departure from chemical equilibrium on ideal performance of a bell nozzle, propellant: $N_2O_4/A-50$, $MR = 2.0$, $P_c = 100$, downstream radius/throat radius, 1.0.

Since

$$\tau_w = F_w/A \quad C_f = 2\tau_w/\rho V^2 \quad (19)$$

the Reynolds number may be written as

$$Re = 144 P_c \{1 + [(\gamma - 1)/2]M^2\}^{[2w(1-\gamma)+1+\gamma]/2(1-\gamma)} \times M(g\gamma)^{1/2}(\mu_c)^{-1}(RT_c)^{-1/2} \quad (20)$$

The expression for nozzle frictional drag is obtained by solving Eqs. (18) and (19) for F_w , and the shear drag loss C_{eD} is

$$C_{eD} = \frac{\text{shear drag} = F_w}{\text{ideal one-dimensional thrust} = C_{F,i} P_c A_i C_D} \quad (21)$$

The viscosity was calculated from $\mu = \mu_c(T/T_c)^w$.

It can be shown that, for nozzles of a given type and area ratio and a gas of a given ratio of specific heats, the drag loss factor C_{eD} is proportional to the parameter FP_c . This parameter is used in presenting the data in Fig. 3.

Chemical Kinetic Effects

A one-dimensional analysis based on the Bray freezing criterion⁴ is used to evaluate nozzle inefficiency caused by incomplete recombination of the dissociated chemical species in the nozzle. The area ratio at which effective composition freezing occurs is computed as a function of propellant, nozzle geometry, and operating conditions. This effective composition freezing point may then be interpreted as a loss in ideal (equilibrium) performance. This is evident from Fig. 1, in which composition freezing area ratio is presented as an arbitrary parameter. The basic method is as follows: From the set of reactions, which actually determine the chemical composition in the nozzle, one must be chosen as dominant on the basis of its high concentration, high heat of reaction and slow rate. In addition to this reaction, as many of the other reactions as are required to adequately describe

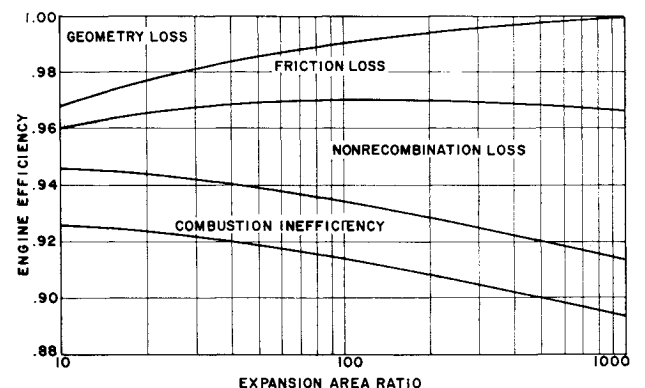


Fig. 5 Loss distribution for typical space engine, $P_c = 100$ psia, $N_2O_4/0.5 N_2H_4 + 0.5 UDMH$, $F = 10K$.

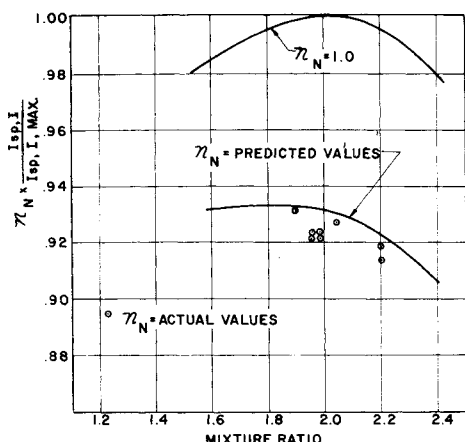


Fig. 6 Comparison of experimental with predicted nozzle efficiency, engine no. 1, propellant: $N_2O_4/A-50$, $P_c = 100$ psia.

the gas composition in the nozzle are considered. Equilibrium expansion composition and flow data are used as a basis to determine when a significant departure from equilibrium should occur.

The diatomic recombination reaction is $A + B + M \rightleftharpoons AB + M$, where M is an inert third body. The rate of recombination is

$$R_f = k_f \prod_{i=1}^J \left(\frac{\rho \gamma_i}{W_T} \right)^{v_i'} \quad (22)$$

The mole fraction of M is taken as 1, i.e., every atom and molecule present is considered equally effective as a third body. The reaction rate constant is assumed to vary with temperature according to the relation

$$k_f = aT^b \exp(c/T) \quad (23)$$

where a , b , and c are constants for each reaction. The required equilibrium rate of composition change along the nozzle is obtained by combining the composition and nozzle geometry data as follows:

$$d\gamma_i/dx = (d\gamma_i/d\epsilon)/(dx/d\epsilon) \quad (24)$$

Composition freezing is assumed to occur when $B = |R_f/X_f|$

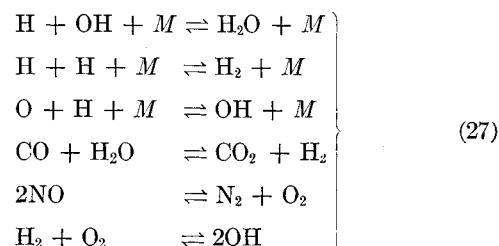
is unity. The value of X_f is determined by solving a set of J simultaneous equations of the form

$$\frac{d\gamma_i}{dx} = \sum_{r=1}^J a_{i,r} X_r \quad i = 1, \dots, J \quad (25)$$

where the coefficients are determined as

$$a_{i,r} = (W_T/\rho V)(v_{ir}'' - v_{ir}') \quad (26)$$

where the number of reactions must equal the number of chemical species considered. The set of reactions chosen to describe the recombination $N_2O_4/0.5 N_2H_4 + 0.5$ UDMH is as follows:



Species used here to solve for X_f are H, OH, O, CO, NO, and H_2 .

The heat evolved by the first reaction is the greatest. Also, the concentrations of H and OH in the chamber as shown by the equilibrium calculations are high when compared with other unrecombined species. Assuming that the second reaction dominant resulted in predicted nozzle losses that were unrealistically high when compared with experimental data, the first was taken as the reaction that determined the freezing point. The forward rate constant of this reaction is, from Ref. 5, $k_f = 4.1 (10)^{13} \text{ ft}^6/\text{lb-mole}^2\text{-sec}$. The flow was assumed to undergo no change in chemical composition from the area ratio at the freezing point to the exit area ratio.

The results of the freezing point calculations are shown in Fig. 4, where C_{eK} , defined as

$$C_{eK} = 1 - \frac{I_{sp} \text{ chemical nonequilibrium}}{I_{sp, I}} \quad (28)$$

is plotted against nozzle exit area ratio. These data are for bell (vacuum Rao) nozzles with 1.0 R_t downstream throat blend radius. At low pressures where composition freezing occurs just downstream of the throat, increasing this blend radius may bring about a reduction in the performance loss.

Table 1 Comparison of predicted and measured efficiencies for several space engines

Propellant:	Engine						
	1 $N_2O_4/A-50^a$	2 $N_2O_4/A-50$	3 $N_2O_4/A-50$	4 IRFNA ^b / UDMH	5 IRFNA/ UDMH	6 $N_2O_4/A-50$	7 $N_2O_4/A-50$
MR	2.0	2.0	2.0	2.8	2.8	2.0	2.0
P_c	100	100	100	206	206	100	100
A_e/A_t	30:1	40:1 (conical)	60:1 (conical)	20:1 (not Rao contour)	40:1 (not Rao contour)	40:1	60:1
c_I^*	5602	5602	5602	5390	5390	5602	5602
$C_{F, I}$	1.912	1.941	1.977	1.830	1.893	1.941	1.977
C^*	4781	5429	5427	4901	4909	5367	5395
η_c	85.3	96.8	96.8	90.9	91.1	95.8	96.3
C_F	1.772	1.776	1.830	1.725	1.807	1.795	1.887
η_N measured	92.7	91.5	92.6	94.3	95.5	92.5	95.4
η_N predicted	92.75	93.15	92.58	95.58	95.51	93.58	94.39
Losses							
Geometry	2.00	1.70	1.70	2.28	2.24	1.75	1.40
Friction	1.55	2.52	2.84	1.20	1.65	1.57	1.62
Recombination	3.70	2.63	2.88	0.40	0.60	3.10	2.54

^a Aerozine -50 (0.5 $N_2H_4 + 0.5$ UDMH).

^b Inhibited red fuming nitric acid.

Experimental Evaluation of Nozzle Stagnation Pressure

A basic problem in evaluating actual rocket engine performance is measuring the true nozzle stagnation pressure. Knowledge of this pressure is required in order to establish combustion efficiency. The use of conventional injector-end pressure taps has been found unsatisfactory in meeting the accuracy requirements of current in-space engines because of radial pressure gradients and the uncertainties of predicting the total pressure loss caused by the heat release in the combustion process. This is particularly true in the case of conical combustion chambers (which have been found desirable for construction with ablatives), since the heat is added to an accelerating stream. It has been found more satisfactory to derive nozzle stagnation or plenum chamber pressure directly from thrust measurements. From Eq. (3) we can write

$$P_c/P_{c, \text{inj}} = F/C_D A_t \eta_N C_F, i P_{c, \text{inj}}$$

A knowledge of the actual nozzle efficiency is required in order to reduce the measured thrust to an effective chamber pressure. In order to minimize the uncertainties, it is best to use a single nozzle of low area ratio. A nozzle of 1:1 area ratio or essentially no (diverging) nozzle at all is preferred. In this case divergence, frictional, and chemical kinetics effects are minimized. The ideal thrust coefficient is actually higher than the one-dimensional value for a 1:1 expansion area ratio, however, since $\epsilon_{\text{eff}} = 1/C_D$, as shown previously. This technique, used to determine the total pressure loss in the chamber for later interpretation of altitude or simulated altitude test data, indicates variations of several percent, depending upon injector efficiency, pattern, and pressure tap location.

Experimental Verification of Nozzle Efficiency

To check the validity of the method developed, a comparison was made between predicted efficiencies and measured efficiencies of those engines for which simulated altitude test data were available. The results of this comparison are summarized in Table 1 where the given chamber pressures are the nominal design values. The test runs selected were those where a consistent body of valid data was available and do not necessarily represent the final production engines. The tabulated data are based upon averages of several test runs. In all of the cases, an attempt was made to base combustion efficiency on the true nozzle total pressure. For the more recent engines designed with conical combustion chambers, combustion efficiency was determined from sea-level tests of the injector in conjunction with a combustion

chamber with a cutoff nozzle. For the older engines where such data were not available, the one-dimensional relationship, which assumes complete heat release at the injector face, was used to establish plenum pressure and combustion efficiency. All of these engines have cylindrical combustion chambers of relatively large characteristic length, making this assumption reasonable. Estimates of nozzle performance losses were made, based upon the techniques given previously. Actual nozzle contours for each engine were used, taking into account variations in the blend radius downstream of the throat and conical sections in some nozzles.

The agreement between predicted and measured nozzle efficiency is good, considering that these tests were not set up with this type of evaluation in mind. The data show clearly that performance losses attributed to nozzle inefficiency are present in low-pressure space engines.

Predicted and actual nozzle efficiencies are shown as functions of propellant mixture ratio in Fig. 6. The optimum mixture ratio, if the flow remains in chemical equilibrium, is seen to be 2.0. However, when the predicted losses are taken into account, the optimum mixture ratio changes to 1.8. This shift is caused by the reduction in dissociation loss that occurs with a decrease in mixture ratio. The experimental points agree fairly well with the predicted curve.

Conclusion

Although additional refinements such as taking into account the effect of combustion efficiency on nozzle efficiency and correlation with data over more widely separated operating conditions are required, the technique presented will enable the prediction of the performance of current in-space engines with good precision. The Bray sudden-freezing criterion provides a useful engineering tool for estimating the loss in nozzle efficiency caused by nonequilibrium expansion.

References

- ¹ Rao, G. V. R., "Exhaust nozzle contour for optimum thrust," *Jet Propulsion* **28**, 377-382 (1958).
- ² Sauer, R., "General characteristics of flow through nozzles at near critical speeds," NACA TM 1147 (1947).
- ³ Rubesin, M. S., Maydew, R. C., and Varge, S. A., "An experimental and analytical investigation of the skin friction of the turbulent boundary layer on a flat plate at supersonic speeds," NACA TM 2305 (February 1961).
- ⁴ Bray, K. N. C. and Appleton, J. P., "Atomic recombination in nozzles: Methods of analysis for flows with complicated chemistry," Dept. of Aeronautics and Astronautics, Univ. of Southampton, England, Rept. AASU-166 (April 1961).
- ⁵ Baier, R. W., Byron, J. R., and Armour, W. H., "Application of the Bray criterion for predicting atomic recombination effects in propulsion systems," Aeronutronic, A Division of Ford Motor Co., Newport Beach, Calif. (February 1962).